Chemical Engineering Journal 103 (2004) 1–5

Chemical Engineering Journal

www.elsevier.com/locate/cej

Power consumption and onset speed for gas induction in a gas-induced contactor

Mousa Jafari, Jafar S. Soltan Mohammadzadeh*

Department of Chemical Engineering, Sahand University of Technology, Tabriz 51335-1996, Iran

Received 13 December 2003; received in revised form 1 June 2004; accepted 17 June 2004

Abstract

In the present work, power characteristics of a gas-induced contactor have been studied. The onset speed for gas induction at different liquid levels has been determined. The effects of impeller speed, gas induction, gassing and liquid level on power consumption have been examined. In this system power number was between 1 and 2 at impeller speeds of 400–1600 rpm. At low impeller speeds, power consumption decreased significantly by gassing (60% drop in power consumption at speed of 800 rpm), while at higher speeds, because of gas induction, effect of gassing on power consumption was not considerable (15% drop at speed of 1600 rpm). For high and same impeller speeds, power consumption of this contactor is lower than that of Rushton and flat blade disk turbine (FBDT) agitated contactors.

Keywords: Power consumption; Gas-induced contactor; Gas induction; Mixing; Hydrodynamics

1. Introduction

Mixing processes have always played a principal role in process industries. Mechanically agitated contactors (MACs) are important components in processing plants in every branch of the chemical industry such as food industry, biotechnology and environmental technology. A significant amount of data can be found in the literature on characteristics and performance of these contactors [1,2]. Agitator and vessel with a six-blade Rushton disc turbine, gas sparger, and four baffles is now a classical design for many applications. However these contactors have disadvantages such as high power consumption and poor top-to-bottom mixing in multiple impeller systems [3]. Recent reports on the hydrodynamics of these systems have shown that other disc turbine agitators can also offer some advantages [3,4].

In many gas–liquid reacting processes, the per-pass conversion of gas is low and the recirculation of the un-reacted gas from the headspace back into the liquid phase is important. This is especially true when a costly and/or potentially hazardous gas such as ozone is involved in the process. This problem may be solved using different reactor designs such as surface aerators, sparged loop reactors or gas-inducing mechanically agitated reactors. A conventional gas-inducing reactor consists mainly of a hollow shaft and impeller or a standpipe with several different types of impellers. The mechanism of gas induction is not yet clearly understood. Several investigations on the design of gas-inducing reactors have been reported in the literature [5–9].

Power consumption is one of the most important parameters in establishing the efficiency of the reactor system. Generally, the power consumption of a MAC is a function of the shape, size, speed and location of the impeller, density and viscosity of the fluid, and the size and geometry of the tank. Determining the power consumption is an important parameter in comparing different impeller designs. Several investigations on power consumption of traditional [9] and newer impellers [4,10] can be found in the literature.

* Corresponding author. Tel.: +98 411 4249604; fax: +98 411 4245770.
E-mail address: soltan@sut.ac.ir (J.S.S. Mohammadzadeh).

1385-8947/$ – see front matter
doi:10.1016/j.cej.2004.06.004

Nomenclature

D	impeller diameter (m)
FBDT	flat blade disc turbine
Fr_c	Froude number at onset speed for gas induction
g	gravitational acceleration (m/s^2)
h	dimensionless height
H	working liquid level (m)
H_D	off-bottom clearance of the top of the draft tube (m)
MAC	mechanically agitated contactor
N	impeller speed (s^{-1})
N_c	onset speed for gas induction (s^{-1})
N_P	power number
N_{Re}	Reynolds number
P	agitation power in the nongassing condition (W)
PBDT	pitched blade downward turbine
P_g	agitation power in the gassing condition (W)
T	tank diameter (m)
V	working liquid volume (m^3)

Greek letters

μ	liquid viscosity (kg/m s)
ρ	liquid density (kg/m^3)
τ	real working torque of the shaft (N m)
τ_0	blank torque of the shaft (N m)

The main purpose of this study is to verify power consumption and gas induction process in a gas-induced contactor, which can be used as an ozonation reactor for wastewater treatment. Hsu and Huang [11,12] reported about performance of a contactor involving two in-series six-blade 45° pitched blade disk turbines (PBDTs) enclosed by a draft tube that could induce the un-reacted gases. In this work, effective parameters on power consumption and onset speed for gas induction have been studied.

2. Experimental setup

All experiments were carried out in a transparent vessel with a flat bottom. Schematic diagram of the experimental setup is shown in Fig. 1. The cylindrical tank body and draft tube were made of Plexiglas. The contactor had an inner diameter of 190 mm, a height of 750 mm, and a wall thickness of 5 mm. The inner diameter, height, and thickness of draft tube were 95, 140 and 2.5 mm, respectively. The off-bottom clearance of the draft tube was 100 mm, however this clearance could be adjusted for optimization experiments using supporting rods. Four baffles with a width of 5 mm were symmetrically installed on the inner wall of the draft tube.

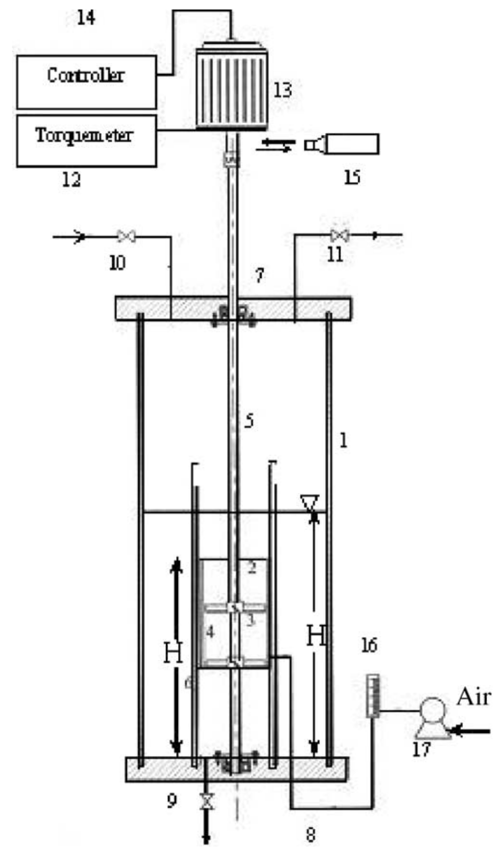

Fig. 1. Schematic diagram of the experimental setup. 1: Tank body; 2: draft tube; 3: PBDT; 4: inner baffles; 5: shaft; 6: support rods; 7: top cap; 8: gas inlet; 9: liquid outlet; 10: liquid inlet; 11: gas outlet; 12: torquemeter; 13: variable-speed motor; 14: speed controller; 15: photo/contact tachometer; 16: gas flowmeter; 17: air compressor.

Two six-blade 45° PBDTs with a diameter of 70 mm were installed on the shaft. The distance between the two impellers was fixed at one impeller diameter (i.e. 70 mm) and the plane of lower turbine was level with the lower end of the draft tube. The outlet of gas pipe was located between two impellers and 15 mm above the lower impeller to directly introduce the fresh gas into the contactor. The liquid inlet and outlet nozzles were installed on the upper and lower caps, respectively. The shaft was driven by an electric motor (120 W, 24 V and 4000 rpm max). The impellers could be operated at different speeds using a speed controller. A photo/contact tachometer was used to measure the impeller speed.

Power input to the impellers was determined using a torque-meter and tachometer in the impeller speed range of 200–1600 rpm. The blank torque (τ_0, N m) and working torque (τ, N m) of the shaft at any impeller speed (N, s^{-1}) in each experiment were substituted into Eq. (1) to obtain the power consumption for agitation (P, W).

$$P = 2\pi N(\tau - \tau_0) \quad (1)$$

3. Results and discussion

3.1. Onset speed for gas induction

The onset speed for gas induction is defined as the impeller speed at which the gas above the liquid surface begins to be sucked into the liquid phase through the draft tube. In order to investigate the onset speed for gas induction, it may be necessary to know flow pattern in the contactor at different impeller speeds. So here, the flow pattern observation at liquid level of 320 mm and at impeller speeds of 200–1600 rpm is briefly reviewed. In the non-gassing condition (i.e. only liquid is mixed in the contactor without gas flow) and at impeller speed of 200 rpm, no liquid vortex was observed around the draft tube. By increasing the impeller speed up to 600 rpm, the main liquid vortex was completed but no gas vortex had yet been formed. At impeller speed of 800 rpm, the central gas vortex was formed at the center of the liquid surface above the draft tube and it came down to the upper impeller. So, the first gas bubbles were sucked into the liquid phase. Increasing impeller speed up to 1100 rpm led to a homogeneous gas–liquid dispersion. This speed is called onset speed for gas induction at liquid level of 320 mm. At this speed, the impellers pulled the gas vortex inward to the draft tube and then disturbed it using the inner baffles and broke it into bubbles. The bubbles were then pulled down and were distributed out of the draft tube by the lower impeller. Only a small amount of bubbles, near the contactor wall, moved spirally upward and escaped the liquid phase. A portion of these bubbles was sucked back into the liquid phase by the central gas vortex. By further increasing the impeller speed no significant variation on flow pattern and gas induction was observed. In the case of gassing condition and at low impeller speeds, the predominant regime was flooding in which gas bubbles moved up through the draft tube without any significant disturbance by the impellers. This regime occurs at low impeller speeds and high gas flow rates. As the speed of impellers was raised above 1000 rpm, a homogeneous gas–liquid dispersion was observed in the contactor. The higher impeller speeds just caused a higher circulation speed and had no considerable effect on the gas–liquid contact regime. From experimental studies, it was found that gas induction depends significantly not only on the impeller speed but also on the impeller diameter and liquid level [12]. Among these parameters, the effect of liquid level on gas induction is presented here. The onset speed experiments were carried out at different liquid levels between 260 and 420 mm. Fig. 2 shows the variation of Froude number at onset speed (Fr_c) as a function of dimensionless height (h):

$$Fr_c = \frac{DN_c^2}{g} \tag{2}$$

$$h = \frac{H - H_D}{T} \tag{3}$$

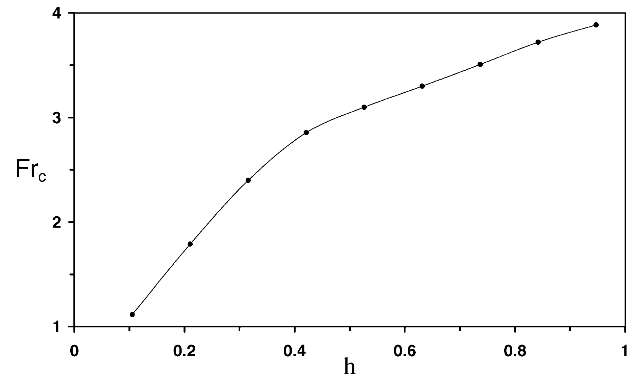

Fig. 2. Variation of Froude number at onset speed vs. dimensionless height.

where D, N_c and g represent the impeller diameter, onset speed and gravitational acceleration, respectively. H, H_D and T express the working liquid level, clearance of top of the draft tube and the tank diameter, respectively. As shown in Fig. 2, Froude number increases by increasing the dimensionless height. The onset speed for gas induction corresponding to any liquid level was obtained using visual observation. The onset speed could be found using power curves, also. Since gas induction leads to a considerable drop in power consumption, the break points on power curves indicate the onset speeds. Hsu and Huang [12] have also carried out the onset speed experiments in a bench-scale gas-induced reactor and correlated the onset speed with the relevant geometric factors. These trends are similar to the reported findings.

3.2. Power consumption

3.2.1. Variation of power consumption at different impeller speeds

In order to study the effect of impeller speed on power consumption, experiments were performed at impeller speeds of 400–1600 rpm and liquid level of 320 mm (liquid volume of 9 L). The dimensionless power number (N_P) and Reynolds number (N_{Re}) are defined as

$$N_P = \frac{P}{\rho N^3 D^5} \tag{4}$$

$$N_{Re} = \frac{\rho ND^2}{\mu} \tag{5}$$

where ρ and μ represent liquid density and liquid viscosity, respectively. Fig. 3 shows the variation of power number as a function of Reynolds number. Because of high range of impeller speeds in this contactor, the range of Reynolds number is quite wide. At these values of Reynolds numbers, the conventional MACs show constant values of power number. This is because of the effects of using baffles on the inner wall of agitated tanks while no baffle was installed on this contactor. As shown in Fig. 3, the power number decreases with an increase in Reynolds number. A similar behavior has been

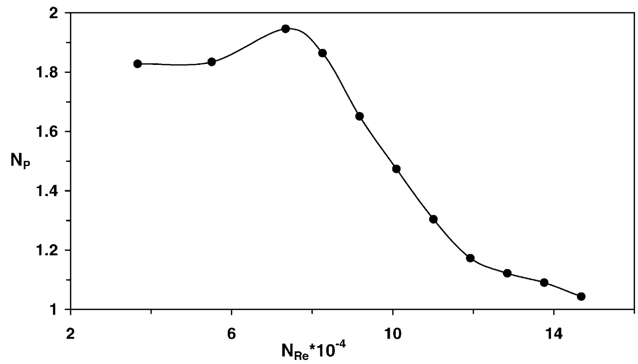

Fig. 3. Power number at different Reynolds numbers.

reported for MACs without baffles [13]. The power number curve has a relative maximum at impeller speed of about 800 rpm. At this speed, gas induction has not yet occurred and the effect of gas induction on power consumption can not be observed.

3.2.2. Effect of gassing on power consumption

When gas is sparged into an agitator at a given impeller speed, the power consumption at this condition (P_g) decreases because of the formation of gas cavities behind the blades [3]. The extent of this reduction in power consumption is not yet fully predictable from basic principles. The key to the prediction of P_g is, understanding formation of the captive cavities of gas which are drawn by centrifugal forces into the roll vortices formed behind the blades. This gas consists of freshly sparged gas and gas re-circulated from the dispersion back into the cavity. In fact, the shape and size of these cavities influence the power consumption at particular speed and gassing rate. The comparison of power consumption in gassing and non-gassing conditions may be more clear using power ratio (P_g/P) which is shown in Fig. 4. As shown, in Fig. 4 the lower the impeller speed the more effective the gassing on power consumption. Experiments show that at impeller speeds lower than 800 rpm, the power ratio falls down to 0.25 (not shown in the figure).

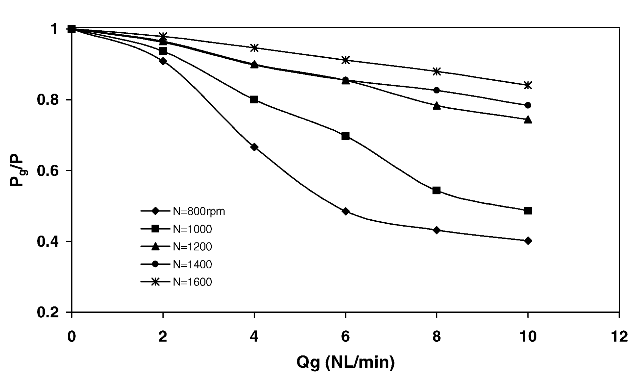

Fig. 4. Gassed to un-gassed power ratio vs. gas flow rate at different impeller speeds.

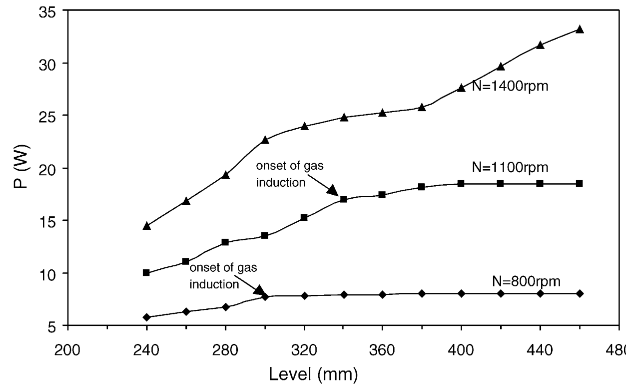

Fig. 5. Power consumption at different liquid levels and impeller speeds.

3.2.3. Effect of liquid level on power consumption

In the gas-induced contactor and at a constant impeller speed, liquid level is limited to the level corresponding to onset speed for gas induction whereas with higher liquid level, the contactor loses its capability of gas induction. In order to verify the effect of liquid level on power consumption, experiments were carried out at liquid levels in the range of 240–460 mm and impeller speeds of 800, 1100 and 1400 rpm. As shown in Fig. 5, at impeller speeds of 800 and 1100 rpm after a specific level, power consumption remains constant. In fact, this level is that of onset speed for gas induction and at higher liquid levels, the impellers cannot form the main liquid and gas vortexes. So, the power consumption is approximately constant. These liquid levels are not practically important since at these levels, the contactor misses its main advantage (i.e. gas induction). These limiting levels increase with an increase in impeller speed. For example, increasing the impeller speed from 800 to 1100 rpm causes a rise in limiting level from 300 to 340 mm. The limiting level corresponding to the speed of 1400 rpm occurs at even higher levels (not shown in the figure).

3.2.4. Comparison of power consumption of gas-induced contactor with MACs

The conventional MACs are generally designed based on specific standard guidelines. Neither baffles nor sparger is used in gas-induced contactor, instead a draft tube and two impellers are used in this type of contactors. Fig. 6 shows a comparison of specific power consumption of gas-induced contactor with a standard FBDT (Rushton) and a standard PBDT contactor. The specific power consumption of this contactor is much lower than that of Rushton contactor. The consumed power of this contactor at optimum operating condition (1100 rpm at which a homogeneous gas–liquid dispersion and the best state of gas induction occurs) is approximately equal to that of standard PBDT contactor. This is a result of not using baffles in gas-induced contactors. The standard PBDT contactor is not capable of gas induction and provisions must be made to recover and recycle the un-reacted gas. Despite the fact that the gas-induced contactor operates at high impeller speeds, its power consumption is not higher

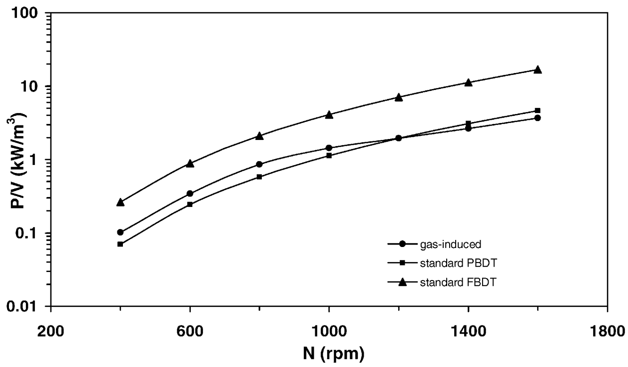

Fig. 6. Comparison of power consumption for gas-induced contactor and Rushton and standard PBDT contactors.

than that of conventional contactors. For example, the power consumption of this contactor operating at impeller speed of 1100 rpm is approximately equal to that of Rushton contactor operating at 700 rpm.

4. Conclusion

In this work, mechanical power consumption and onset speed for gas induction have been studied and reported for a gas-induced contactor. The experiments show that the power number is between 1 and 2 at impeller speeds of 400–1600 rpm and it decreases with an increase in impeller speed because of not using any baffles. The gassing leads to a considerable drop in power consumption especially at low speeds. At speeds higher than 1000 rpm because of gas induction, the effect of gassing on power consumption is not significant. At liquid levels higher than limiting level, the power consumption remains almost constant. Despite the fact that a gas-induced contactor requires a high impeller speed to initiate gas induction, it consumes less power compared to the conventional gas–liquid contactors.

References

[1] B.B. Breman, A.A.C.M. Beenackers, M.J. Bouma, Flow regimes gas hold-up and axial gas mixing in the gas-liquid multi-stage agitated contactor, Chem. Eng. Sci. 50 (18) (1995) 2963–2982.
[2] A.W. Patwardhan, J.B. Joshi, Design of stirred vessels with gas entrained from free liquid surface, Can. J. Chem. Eng. 76 (1998) 355–364.
[3] N. Harnby, M.F. Edwards, A.W. Nienow, Mixing in the Process Industries, Butterworth Heinemann, London, 1997.
[4] A.W. Nienow, Gas-liquid mixing studies: a comparison of Rushton turbines with some modern impellers, Inst. Chem. Eng. 70 (1996) 417–423.
[5] K. Saravanan, V.D. Mundale, J.B. Joshi, Gas inducing type mechanically agitated contactors, Ind. Eng. Chem. Res. 33 (1994) 2221–2240.
[6] V.D. Mundale, J.B. Joshi, Optimization of impeller design for gas inducing type of agitated contactors, Can. J. Chem. Eng. 73 (1995) 6–17.
[7] J.B. Joshi, Modification in the design of gas inducing impellers, Chem. Eng. Commun. 5 (1980) 109–114.
[8] S.S. Patil, J.B. Joshi, Stability of gas-inducing type impellers, Can. J. Chem. Eng. 77 (1999) 793–803.
[9] Cz. Kuncewicz, M. Pietrzykowski, Hydrodynamic model of a mixing vessel with pitched-blade turbines, Chem. Eng. Sci. 56 (2001) 4639–4672.
[10] M. Bouaifi, M. Roustan, Power consumption, mixing time and homogenisation energy in dual-impeller agitated gas-liquid reactors, Chem. Eng. Process. 40 (2001) 87–95.
[11] Y.C. Hsu, C.J. Huang, Characteristics of a new gas-induced reactor, Am. Inst. Chem. Eng. J. 42 (11) (1996) 3146–3152.
[12] Y.C. Hsu, C.J. Huang, Ozone transfer with optimal design of a new gas-induced reactor, Am. Inst. Chem. Eng. J. 43 (9) (1997) 2336–2342.
[13] R.E. Treybal, Mass Transfer Operation, third ed., McGraw-Hill, New York, 1990.